Supporting Information

Xu et al. 10.1073/pnas.1211762109

SI Materials and Methods

Cell Lines. All cells were maintained at 37 °C and 5% CO_2, and cultured in DMEM/Ham's Nutrient Mixture F-12 supplemented with 10% FBS and 1% penicillin/streptomycin (all concentrations by volume). Hek293 cells stably expressing MC4R, CCK2R, or both were described for testing binding affinities of heterobivalent ligands (1). The parental cell line used in the current study was human colorectal carcinoma, HCT116 (American Type Culture Collection; CCL 247). HCT116 cells stably expressing MC1R (HCT116/MC1R), expressing CCK2R (HCT116/CCK2R), or expressing both MC1R and CCK2R (HCT116/MC1R/CCK2R) were made in our laboratory. Briefly, HCT116 cells were transfected with the pCMV6-Entry Vector containing human melanocortin 1 receptor (Origene; RC 203218) by using FuGENE 6 transfection reagent (Roche; 1814-443) and a stable transfectant was selected under the selective media including 0.4 mg/mL geneticin (Life Technologies; 11811-031). A stable HCT116/CCK2R cell line was made by transfecting HCT116 cells with CCK2R construct (1) and selected under the selective media including 0.2 mg/mL zeocin (Invitrogen; 450430), whereas a stable dual receptor expressing cell line (HCT116/MC1R/CCK2R) was made by transfecting HCT116/MC1R cells with the CCK2R construct and selected under the dual selective media (0.4 mg/mL geneticin and 0.2 mg/mL zeocin). Three stable HCT116 cell lines were characterized for the expression of target receptors (MC1R and CCK2R) by the ligand-receptor binding assay, Western blotting, and immunocytochemistry staining.

Ligands Synthesis and Fluorescent Labeling. N^{α}-Fmoc protected amino acids, HBTU, and HOBt were purchased from SynPep or from Novabiochem. Rink amide Tentagel S resin was acquired from Rapp Polymere. HOCt, DIC, and DIEA were purchased from IRIS Biotech. The following side chain protecting groups were used for the amino acids: Arg(N^{g}-Pbf); Asp (O-*t*Bu); Glu(O-*t*Bu); His (N^{im}-Trt); Ser(*t*Bu), Trp(N^{i}-Boc); Lys(N^{ε}-Mtt). Cy5-NHS ester was acquired from Amersham Biosciences. Diglycolic anhydride and 4,7,10-trioxa-1,13-tridecanediamine were acquired from TCI America. Bromophenol Blue was acquired from EMD Biosciences. Diethylenetriaminepentaacetic dianhydride was purchased from Sigma-Aldrich. Peptide synthesis solvents, dry solvents, and solvents for HPLC were reagent grade, were acquired from VWR or Sigma-Aldrich, and were used without further purification unless otherwise noted. All of the peptides were manually assembled by using 5- to 50-mL plastic syringe reactors equipped with a frit, and Domino manual synthesizer was obtained from Torviq. The C-18 Sep-Pak Vac RC cartdridges for solid phase extraction were purcahsed from Waters.

Heteromultivalent ligands were synthesized on Tentagel Rink amide resin (initial loading: 0.2 mmol/g) by using N^{α}-Fmoc protecting groups and a standard DIC/HOCt or HBTU/HOBt activation strategy. The resin was swollen in THF for an hour, washed with DMF, and Fmoc protecting group removed with 20% piperidine in DMF (2 min washing, then 20 min). The resin was washed with DMF (3×), DCM (3×), 0.2 M HOBt in DMF (2×), and finally with DMF (2×) and the first amino acid coupled by using preactivated 0.3 M HOCt ester in DMF (3 eq. of N^{α}-Fmoc amino acid, 3 eq. of HOCt, and 3 eq. of DIC). An on-resin test using Bromophenol Blue was used for qualitative and continuous monitoring of reaction progress. To avoid deletion sequences and slower coupling rate in longer sequences, the double coupling was performed at all steps with 3 eq. of amino acid, 3 eq. of HBTU, and 6 eq. of DIEA in DMF. A third coupling was performed with symmetric anhydride method (2 eq. of amino acid and 1 eq. of DIC in dichloromethane) wherever beads still tested Kaiser positive. Any unreacted NH_2 groups on the resin thereafter were capped by using an excess of 50% acetic anhydride in pyridine for 5 min. When the coupling reaction was finished, the resin was washed with DMF, and the same procedure was repeated for the next amino acid until all amino acids were coupled. For PEGO spacer introduction, the N-terminal of the peptide on resin was coupled with the glycolic acid spacer by using 10 eq. of diglycolic anhydride in DMF for 5 min. The resin was washed with DMF (3×), with the last washing with dry DMF, and the free carboxylic groups were activated by using 10 eq. of carbonyldiimidazole in dry DMF for 30 min. The resin was washed with dry DMF (3×), and the PEG diamine was coupled by using 20 eq. of 4,7,10-trioxa-1,13-tridecanediamine in dry DMF for 30 min (vigorous vortexing for first 5 min). The resin was washed with DMF, DCM, and THF and dried. A cleavage mixture (10 mL/g resin) of TFA (82.5%), water (5%), triisopropylsilane (5%), thioanisole (5%), and ethanedithiol (2.5%) was injected into the resin and stirred for 3 h at room temperature. The crude peptides were isolated from the resin by filtration, the filtrate was reduced to low volume by evaporation using a stream of nitrogen, and the peptides were precipitated in ice-cold diethyl ether, washed several times with ether, dried, dissolved in water and lyophilized to give off-white solid powders that were stored at −20 °C until purified. The final compounds were purified by size-exclusion chromatography and RP-HPLC and characterized by ESI-MS and/or MALDI-TOF, and/or FT-ICR.

For labeling of ligands with fluorescent and lanthanide tags, Fmoc-Lys (Mtt)-OH (Mtt: methyltrityl) was introduced in the linker region. After the first PEGO linker incorporation, an N^{α}-Fmoc-N^{ε}-Mtt protected lysine was incorporated into the sequence and the peptide synthesis continued to the end as above; the peptide was then cleaved from the resin and purified by using preparative HPLC. For Cy5 labeling, the peptide was cleaved from the resin (using cleavage mixture described above; Mtt group is simultaneously deprotected during cleavage), purified with preparative HPLC, and the labeling was carried out in solution. The purified peptide with free lysine side chain was dissolved in DMSO, 1.2 eq. of commercially available Cy5-NHS ester was added, and the reaction was monitored by using analytical HPLC at 280 nm. Finally, the labeled peptide was separated by using size exclusion chromatography and lyophilized to yield a blue amorphous final product. For Europium (Eu)–chelate complex, the orthogonal Mtt protection from N^{ε} amino group was removed with 5% TFA and 5% Triisopropylsilane in DCM (7×). The DTPA chelator was attached to the free lysine side chain with a short PEG (9 atoms) spacer (Fmoc-Ado-OH) by using HOCt coupling protocol. Using an in situ HOBt ester method, DTPA dianhydride dissolved in DMSO was treated with HOBt for 20 min to obtain di-HOBt ester, which was coupled to the free ε-amino groups on resin. The resin was washed with DMSO, THF, THF-water (1:1), THF, and DCM. After cleavage, the peptides were purified by reverse-phase HPLC and chelate labeled with Eu (III) chloride (3 eq.) in neutral pH buffer. The excess of metal salt was then removed by solid-phase extraction to yield purified compound that was characterized by high resolution ESI-MS, and/or MALDI-TOF, and/or FT-ICR.

Molecular Modeling for htMVL 1 and htMVL 2. Conformational searches and molecular dynamics were performed with Macro-

model version 9.1 implemented under Maestro 7.5 interface on a Linux workstation, using MacroModel implementations of Merck Molecular Force Field (MMFF), AMBER*, and OPLS all-atom force fields. For solution phase calculations, the GB/SA continuum model for water was used. Amide bonds were required to be *trans* except in case of prolines whose imide bonds were intentionally sampled and accepted with either *cis* or *trans* geometry in the conformational searches. Conformational searches were performed with systematic Monte Carlo method of Goodman and Still. Initial conformer populations of $[PG]_3$, PEGO linker, MSH, and CCK ligands were generated. For each search, 5,000 starting structures were generated and minimized until the gradient was less than 0.05 kJ/mol/Å, using the truncated Newton-Raphson method implemented in MacroModel. Duplicate conformations and those with energy greater than 50 kJ/mol above the global minimum were discarded. The complete ligand was then assembled from these minimized conformers and simulated by using molecular dynamics. Molecular dynamic simulations were performed at 300 K with Monte Carlo/Stochastic Dynamics (MC/SD) hybrid simulation algorithm with either the AMBER* all-atom force field or the new OPLS-2005 force field in MacroModel 9.1. A time step of 1.5 fs was applied. The MC part of the algorithm used random torsional rotations between ± 60° and ±180° that were applied to all rotatable bonds except the proline imide C-N bond where the random rotations between ±90° and ±180° were applied. No torsion rotations were applied to bonds in the pyrrolidine ring of proline as the barriers are low enough to permit adequate sampling from the SD part of the simulation. The total simulation time was 10 ns, and 10,000 samples were taken (Fig. 1 *B–D*).

Western Blotting. Cells were lysed in RIPA lysis buffer (50 mM Tris·HCl at pH 7.5, 150 mM NaCl, 0.5% sodium deoxycholate, 0.1% SDS, 1% Nanidet P-40, 1 mM NaF, 1 mM Na_3VO_4, 0.5 mM phenylmethylsulfonyl fluoride, and 10 μg/mL for each of leupeptin, aprotinin, and pepstatin) for 30 min on ice, and then the lysates were centrifuged at 10,000 × g for 10 min at 4 °C. The protein concentration of the supernatant was quantified by using BCA protein assay kit (product no. 23225, Thermo Scientific). Aliquots of protein (40 μg) were subjected to electrophoresis on 10% Tris-Glycine gels (catalog no. EC60785BOX; Invitrogen) containing 0.1% SDS, followed by electrophoretic transfer onto nitrocellulose membranes (catalog no. 162–0115; Bio-Rad). The membranes were then incubated with primary antibody: mouse anti-human CCK2R polyclonal antibody (1:500; ab 43404, Abcam) and rabbit anti-human MC1R polyclonal antibody (1:500; catalog no. GTX108190, GeneTex). To monitor equal protein loading, membranes were also probed for GAPDH by using rabbit anti-GAPDH polyclonal antibody (1:1,000; Santa Cruz). For visualization, horseradish peroxiase (HRP)-conjugated secondary antibodies: Goat anti-rabbit IgG HRP and goat anti-mouse IgG HRP, followed by ECL kit (catalog no. 32209, Thermo Scientific) were used.

Immunofluorescence Analysis. Cells were cultured on glass coverslips placed at the bottom of culture wells and fixed with cold methanol:acetone (1:1) for 10 min. Plates were washed with ice cold PBS and incubated with 1% BSA in PBST for 30 min to block unspecific binding of the antibodies. Cells were then treated with primary antibodies including MC1R anti-rabbit polyclonal antibody (1:300; AMR-020, Almone Labs) and CCK2R anti-mouse polyclonal antibody (1:300; AB43404, Abcam), followed secondary antibody treatments (1:2,000; Alexa Fluor 555 donkey anti-rabbit IgG and 1:2,000; Alexa Fluor 488 donkey anti-mouse IgG, Invitrogen). Coverslips were mounted with mounting medium containing DAPI (Vector Laboratories). Micrographs were taken with a Leica DMI6000 inverted microscope, TCS SPS tantem confocol scanner, through a 63×/1.40 N.A. Plan Apochromat oil immersion objective lens (Leica Microsystems). The 405 Diode (DAPI), 488 tunable argon (Alexa 488) and 543 diode (Alexa 555) laser were applied to excite the samples and tunable emissions were used to eliminate crosstalk between fluorochromes in the Moffitt Analytic Microscopy Core Facility. Images were subsequently acquired at 100 Hz by using dual photomultiplier tube detectors and LAS AF software version 2.1.0 (Leica Microsystems).

Immunohistochemical (IHC) Staining. After fluorescence imaging was performed at 48 h after injection of htMVL 1 or the mice were treated with htMVL 2 for 4, 24, and 48 h, the mice were euthanized and tumors were excised, one core in 10% neutral buffered formalin, the remainder flash frozen in liquid nitrogen and stored at −80 °C. For IHC anlysis, tumor sections were prepared and stained with antibodies in the Moffitt Tissure Core Histology Facility. Tumor samples were stained with hematoxylin/eosin (H&E), rabbit MC1R polyclonal antibody, 1:200 dilution, (GTX70735; GeneTex), goat CCK2R polyclonal antibody, 1:25, (ab77077; Abcam), and rabbit CD31 primary antibody, 1:400, (ab28364; Abcam). The slides were scanned in the Moffitt Analytic Microscopy Core Facility by using an Aperio ScanScope XT digital slide scanner.

Flow Cytometry. Cells were incubated with vehicle or 10 nM Cy5 htMVL 1 for 15 min, followed immediately by a wash step with PBS three times, and then cells were harvested from the cell culture plate going to the sterile tube for the flow cytometry analysis. Cells were sorted and data were analyzed by using FACSAria cell sorter/analyzer (BD Biosciences) in the Moffitt Flow Cytometry Core Facility.

***In Cyto* Lanthanide-Based Time-Resolved Fluorometry and Receptor Density Determination.** The ligand binding affinities of Cy5-labeled ligand (htMVL 1) and Eu-labeled ligand (htMVL 2) were tested on live Hek293/MC4R, Hek293/CCK2R, or Hek293/MC4R/CCK2R cells by using lanthanide-based time-resolved fluorometry (TRF) as described (1). Saturation binding of htMVL 2 was performed by adding a series of diluted htMVL 2 compounds as a total binding and adding excess unlabeled ligands (10 μM NDP-α-MSH or/and 1 μM CCK8) (ligand 3 or/and 4; Fig. S1*B*) as a nonspecific binding. Specific binding was determined by the difference between total and nonspecific binding (Table 1). Competitive binding of Cy5-labeled compound htMVL 1 was conducted by competing Eu labeled monovalent ligands, such as 10 nM Eu-NDP-α-MSH or 1 nM Eu-CCK8 (ligand 5 or 6; Fig. S1*B*) for MC4R or CCK2R, respectively (Table 1). To compare bivalent and monovalent binding models, the compounds were assayed in cells expressing both (bivalent) or one (monovalent) of the corresponding receptors (Table 1). Furthermore, to control for differences in receptor numbers that existed between dual- (Hek293/MC4R/CCK2R) and single-receptor cells (Hek293/MC4R or Hek293/CCK2R), affinities were also assessed in the dual receptor cell line (Hek293/MC4R/CCK2R) in the absence (bivalent) or presence (monovalent) of blocking agents for each receptor in turn (Table 1).

For characterization of HCT116/MC1R/CCK2R, HCT116/MC1R, and HCT116/CCK2R cells, TRF saturation binding assays were conducted by using monovalent ligands, Eu-NDP-α-MSH, or Eu-CCK8 as a total binding, and adding 10 μM NDP-α-MSH or 1 μM CCK8 as a nonspecific binding for MC1R or CCK2R, respectively. Receptor density per cell for each cell line was characterized from the B_{max} values generated by TRF saturation binding assays as described (1) (Fig. S2).

Binding data were analyzed by nonlinear regression analysis by using GraphPad Prism (GraphPad Software). Saturation binding data were fitted to a classic one site binding (hyperbola) equation and competitive binding data were fitted to a classic one-site binding competition equation. For saturation binding assays, K_d

values were determined after correction for nonspecific binding as the concentration that yielded half-maximal binding. For competitive binding assays, the IC_{50} was determined after correction for nonspecific binding as the concentration of unlabeled ligand sufficient to compete off 50% of the labeled ligand.

Live Cell Imaging. For the dose–response assessment of the ligand Cy5 htMVL 1 binding, cells were seeded on sterilized 18-mm–diameter glass coverslips in 12-well plates (3×10^5 cells per well) and incubated overnight at 37 °C. Afterward, the cells were washed with PBS and incubated with the ligand at various concentrations for 15 min at 37 °C, subsequently washed with PBS three times, then imaged. The nuclei were stained with 5 μM Hoechst 33342 (H3570; Invitrogen). For the blocking study, HCT116/MC1R/CCK2R cells were cotreated with 10 nM htMVL 1 and blocking agents (10 μM NDP-α-MSH only, 10 μM CCK8 only, or both) for 15 min, immediately washed with PBS, then imaged. For the internalization of htMVL 1 conjugates, cells were treated with 50 nM of the ligand at various time points at 37 °C, subsequently washed with PBS to remove unbound conjugates, and then imaged.

Images were acquired by using Zeiss Z1 Observer microscope (Carl Zeiss) equipped with a 40× 1.3 N.A. objective lens and an EXFO x-cite 120 xenon as the excitation light source. The Cy5 fluoresecence excitation filter is a band pass 640/30, and the emission filter is a band pass 690/50. An axiocam MRM3 camera (Carl Zeiss) was used to acquire images. Five random fields were imaged per sample and the fluorescence intensity in that field was calculated by using the software of Definiens. Cy5-positive cells were determined after correction for autofluorescence background (the intensity of 250 or less). For each experimental condition, a total of 600∼800 cell numbers were quantified for the fluorescence intensity per cell and the Cy5-positive cell percentage. Some of the representative images were adjusted for brightness and contrast by using CoreDRAW Graphics Suite X4 and Irfanview software.

Subcellular Localization of htMVL 1. Axial through-focus image sets were acquired for the Cy5 tagged ligand, htMVL1, then the selected organelle specific probe using 3D-deconvolution microscopy (Fig. S4*C*). Image deconvolution was performed by using empirically derived point spread functions, and an iterative algorithm, as described (2, 3). The location of the plasma membrance or lysosomes were determined by loading with either FM 1–43 (Invitrogen; T-35356) or LysoSensor yellow/blue DND-160 (Invitrogen; L-7545), respectively, immediately before image acquisition. Fluorophore specific filter sets were used to delineate signals from each probe.

Animals. Female nu/un mice (6∼8 wk) from Harlan were used in this animal study. Tumor xenografts were generated with engineered HCT116 human colon carcinoma. Cells (5×10^6) were injected s.c. into the right flank (HCT116/MC1R/CCK2R cells) and left flank (HCT116/MC1R or HCT116/CCK2R cells).

In Vivo Fluorescence Imaging. Imaging experiments were done on nu/nu mice bearing HCT116/MC1R/CCK2R and HCT116/MC1R or HCT116/CCK2R tumors by using an IVIS imaging system, 200 Series (Caliper Life Sciences) equipped with a 615- to 665-nm excitation filter and a 695- to 770-nm emission filter. Tumors were measured approximately 0.5–1.0 cm in diameter (14∼21 d after implantation) at the time of imaging. To determine the optimal dose of the htMVL 1 treatment for the tumor-bearing mice to visualize the difference between target and control tumors, a series of concentrations of the ligand ranging from 0.5 nmol to 7.5 nmol per mouse were examined and analyzed for selectivity of Cy5 fluorescence signals. For the pharmacodynamic studies, the mice received tail vein injection of 2.5 nmol htMVL 1 in 100 μL of PBS, were anesthetized under 3–4% isoflurane and imaged at various time points after injection. For the blocking experiments, mice received 50 nmol NDP-α-MSH (block 1), 50 nmol CCK8 (block 2), or both NDP-α-MSH and CCK8 (block 3) 30 min before the injection of 2.5 nmol Cy5 htMVL 1, then were imaged at 4 h after injection to acquire blocking images. We acquired all fluorescence images by using the auto exposure instrument setting (Living Image 3.2 software). We subtracted instrument background signal by using an image acquired from an empty stage and subtracted autofluorescence background signal using sham (PBS) treated animals. Following background subtraction, image data were converted to normalized surface radiance (photons per $s/cm^2/sr$) units for cross-comparison of all acquisitions. To determine mean tumor surface radiance, we drew regions of interest over the tumors.

For biodistribution studies, we acquired in vivo images and euthanized animals 4 h after injection. Tumors, organs, and muscle tissue were excised and imaged as described above by using the IVIS 200 system. We subtracted instrument fluorescence background as described above and autofluorescence background by using image data of corresponding tissue from the PBS-treated animals. The mean surface radiance was determined for each tumor and organ.

Ex Vivo Lanthanide-Based TRF. Cells were injected s.c. into the right flank (HCT116/MC1R/CCK2R) and left flank (HCT116/MC1R or HCT116/CCK2R) of nu/nu mice. After ∼2 wk of growth, tumor xenografts reached certain size (0.5–1.0 cm in diameter) and mice were injected via tail vein with 2.5 nmol or 0.5 nmol Eu htMVL 2 or PBS as an auto fluorescence background control. Eu htMVL 2 was diluted in 100 μL of PBS for the injection per mouse. Four, 24, and 48 h after the injection, mice were euthanized by standard CO_2 asphyxiation, tumors and tissues were harvested, one section of tumors in 10% neutral buffered formalin for IHC staining, and the remainder was flash frozen in liquid nitrogen and stored at −80 °C. One section of tumors or tissues was weighed to the nearest milligram on an analytical balance (Fisher Scientific Accu-64 scale). The tumors were homogenized in enhancement solution (1244-105; PerkinElmer) at 20∼100 mg (wet weight)/mL. Homogenates were maintained overnight at 4 °C, diluted in enhancement solution to 5 mg/mL and mixed at room temperature for 30 min. The suspensions were clarified by centrifugation (1,000 × g, 10 min) and 200 μL of supernatants in triplicates for each sample were pipetted into wells of a 96-well microtiter plate. The plates were read on a Victor X4 instrument (2030 Multilabel Reader; PerkinElmer) by using the standard Eu TRF measurement (340 nm excitation, 400 μs delay, and emission collection for 400 μs at 615 nm) on which the total fluorescence of Eu per mg of tissue was determined for each sample. The background fluorescence of tissue homogenates from mice injected with PBS ranged from 1,500 to 2,500 counts per mg of tissue when measured with TRF. The specific Eu fluorescence of tissue homogenates was determined by subtracting background counts from total counts from mice injected with htMVL 2.

For the blocking experiments, tumor-bearing mice received 50 nmol NDP-α-MSH (block 1), 50 nmol CCK8 (block 2), or both NDP-α-MSH and CCK8 (block 3) 30 min before the injection of 0.5 nmol Cy5 htMVL 2 and were euthanized at 4 h after injection. Target tumors (HCT116/MC1R/CCK2R) were harvested and measured for Eu count per mg of tumor as described above.

To ensure the equal delivery of htMVL 2 to the target and control tumor xenografts for each mouse, tumor size was well monitored every other day. To obtain accurate quantitative data with the Eu compounds, the mice with equal size of a pair of tumors were selected for the Eu assays. Furthermore, tumors were excised at certain time after treatments for the measurements of Eu amounts and also processed for IHC staining with

MC1R, CCK2R, and CD31 antibody (Fig. S4*A*). CD31 staining provided important information to show similar vasculature for demonstrating the equal delivery.

Mathematical Modeling for ex Vivo Measurement of htMVL 2. A compartmental model was established with three compartments: blood, experimental tumor simulating HCT116/MC1R/CCK2R cells, and control tumor simulating HCT116/MC1R or HCT116/CCK2R cells. Exchange was allowed between each tumor compartment and blood. Excretion/degradation from the blood was modeled with a first-order rate. Receptor-ligand binding was modeled as in Caplan and Rosca (4) for each tumor compartment. htMVL 2 was also modeled to bind nonspecifically to matrix and/or cells in each tumor compartment. Mathematical modeling full Matlab code is appended to these methods (Dataset S1).

The model generated 13 ordinary differential equations of concentrations of various forms of the htMVL 2 varying with respect to time. These results were solved by using Matlab (Mathworks) with an ordinary differential equation solver. As many parameters were set based on experimental data as possible: CCK2R in experimental tumor was set to be 18 times that of MC1R, CCK2R in control tumor was set to zero, MC1R in control tumor was set to be 24 times that of MC1R in experimental tumor (Fig. S2), affinity of MSH ligand was set to 381.4 nM, affinity of CCK ligand was set to 31.3 nM (Table 1), and the binding enhancement factor was set to 200 based on work by Shewmake et al. (5). Other parameters were fit to the data by hand (it was not possible to use a least squares fitting algorithm because of the nonlinearity of the model): excretion/degradation rate, transfer rate from blood to tumor, transfer rate from tumor to blood, ratio of tumor volume to total body fluid volume, associate rate of MSH, association rate of CCK ligand, nonspecific binding association, nonspecific binding affinity, and the effective concentration of MC1R receptor in experimental tumor.

Model results were plotted by summing all forms of htMVL 2 in experimental tumor (bound and unbound) and in control tumor (Tables S2 and S3). Fold enhancement was determined by dividing the total htMVL 2 content in the experimental tumor by the total htMVL 2 content in the control tumor.

1. Xu L, et al. (2009) Enhanced targeting with heterobivalent ligands. *Mol Cancer Ther* 8(8):2356–2365.
2. Scriven DR, Lynch RM, Moore EDW (2008) Image acquisition for colocalization using optical microscopy. *Am J Physiol Cell Physiol* 294(5):C1119–C1122.
3. Carrington WA, et al. (1995) Superresolution three-dimensional images of fluorescence in cells with minimal light exposure. *Science* 268(5216):1483–1487.
4. Caplan MR, Rosca EV (2005) Targeting drugs to combinations of receptors: A modeling analysis of potential specificity. *Ann Biomed Eng* 33(8):1113–1124.
5. Shewmake TA, Solis FJ, Gillies RJ, Caplan MR (2008) Effects of linker length and flexibility on multivalent targeting. *Biomacromolecules* 9(11):3057–3064.

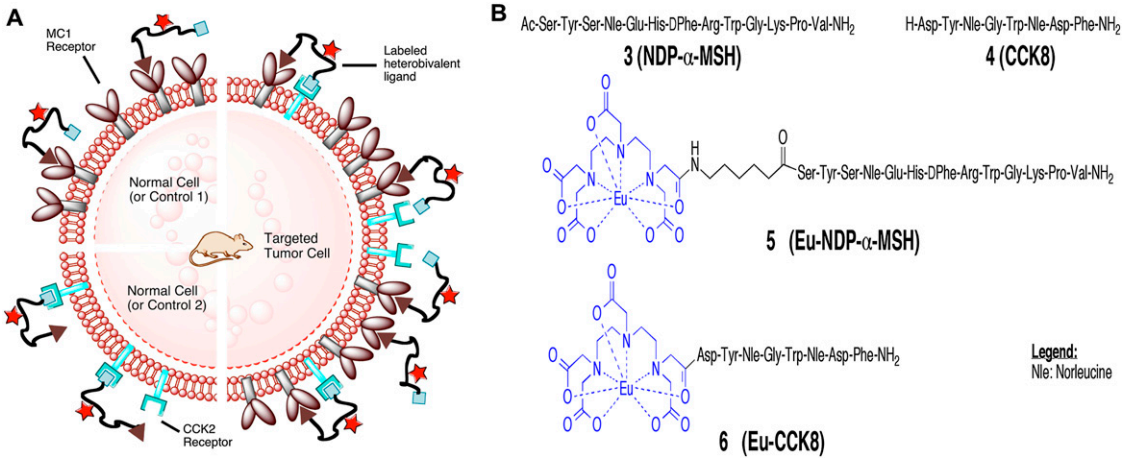

Fig. S1. (*A*) Targeting cell-surface receptor combinations with heteromultivalent ligands. A heterobivalent ligand would bind with high avidity to cells bearing both cognate receptors (targeted tumor tissues) while its binding to cells with only one of these receptors will be very weak (control cells or normal body tissues), with a predicted differential of 10–100 fold. Thus, a high degree of specificity can be achieved in this context therefore leading to the effective delivery of therapeutic or imaging agents to target tumors. Moreover, using two receptor combinations raises the number of potential targets to approximately 2.9 million compared with ~2,500 possible cell surface receptor targets. With "n" receptors assembled into set sizes of "x," the number of combinations is: # = n!/[(n-x)!x!] ~ [nx/x!]. (*B*) Chemical structures of the ligands used in this study. Ligand 3 (NDP-α-MSH), monovalent ligand binding to MC1R or MC4R receptors; Ligand 4 (CCK8), monovalent ligand binding to CCK2R receptors; Ligand 5 (Eu-NDP-α-MSH), Eu-labeled monovalent ligand of NDP-α-MSH; Ligand 6 (Eu-CCK8), Eu-labeled monovalent ligand of CCK8.

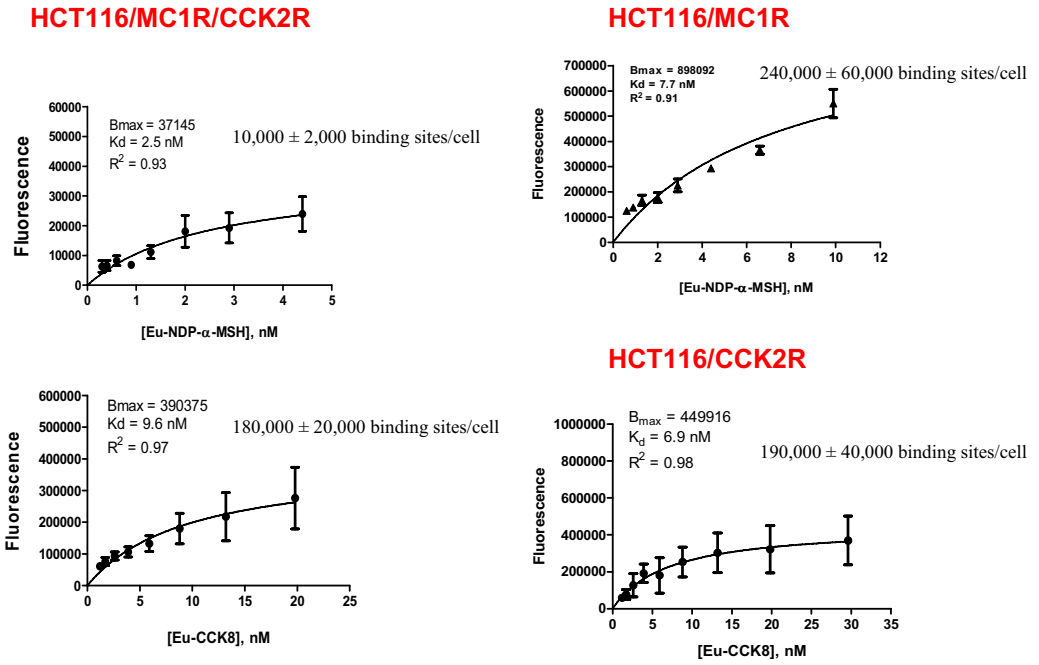

Fig. S2. Representative receptor-ligand binding assays in the engineered stable tumor cell lines. Target cells (HCT116/MC1R/CCK2R) and control cells (HCT116/MC1R or HCT116/CCK2R) were characterized by saturation binding assays (*SI Materials and Methods*) in which total binding was determined by increased concentration of monovalent ligands Eu-NDP-α-MSH and Eu-CCK8 for MC1R and CCK2R receptor, respectively, whereas nonspecific binding was determined in the presence of 10 μM unlabeled NDP-α-MSH or 1 μM CCK8. Specific binding was determined by the difference between total and nonspecific binding.

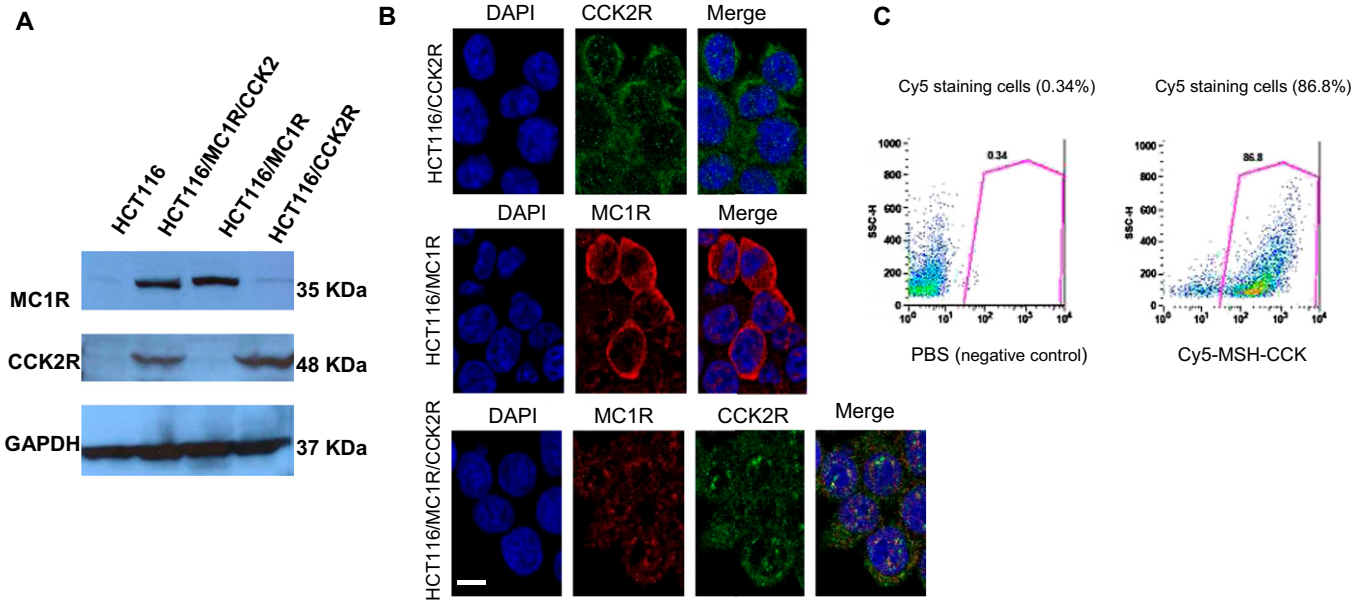

Fig. S3. (*A*) Characterization of engineered stable tumor cell lines by Western blotting. Proteins were harvested from target, control, and parental cells and subjected to immunoblotting analysis. Both MC1R (molecular mass 35 kDa) and CCK2R (molecular mass 48 kDa) proteins were observed in HCT116/MC1R/CCK2R cells, whereas MC1R or CCK2R proteins were only detected in HCT116/MC1R or HCT116/CCK2R cells, respectively. GAPDH was displayed in four cell types as an internal control. (*B*) Characterization of engineered stable tumor cell lines by immunofluorescence staining. Confocal micrograph of cells incubated with the nuclear marker DAPI, MC1R, and CCK2R antibody. MC1R or CCK2R immunolabeling was observed on the cell surface in HCT116/MC1R or HCT116/CCK2R cells, respectively, whereas both MC1R and CCK2R antibody staining was present in HCT116/MC1R/CCK2R cells. (Scale bar: 10 μm.) Negative control samples without primary antibodies were devoid of signal. (*C*) Representative image of FACS sorting. Target cells (HCT116/MC1R/CCK2R) were stained with PBS or Cy5-MSH-CCK ligand (htMVL 1). Percentage of Cy5-positive cells measured by flow cytometry analysis (*SI Meterials and Methods*).

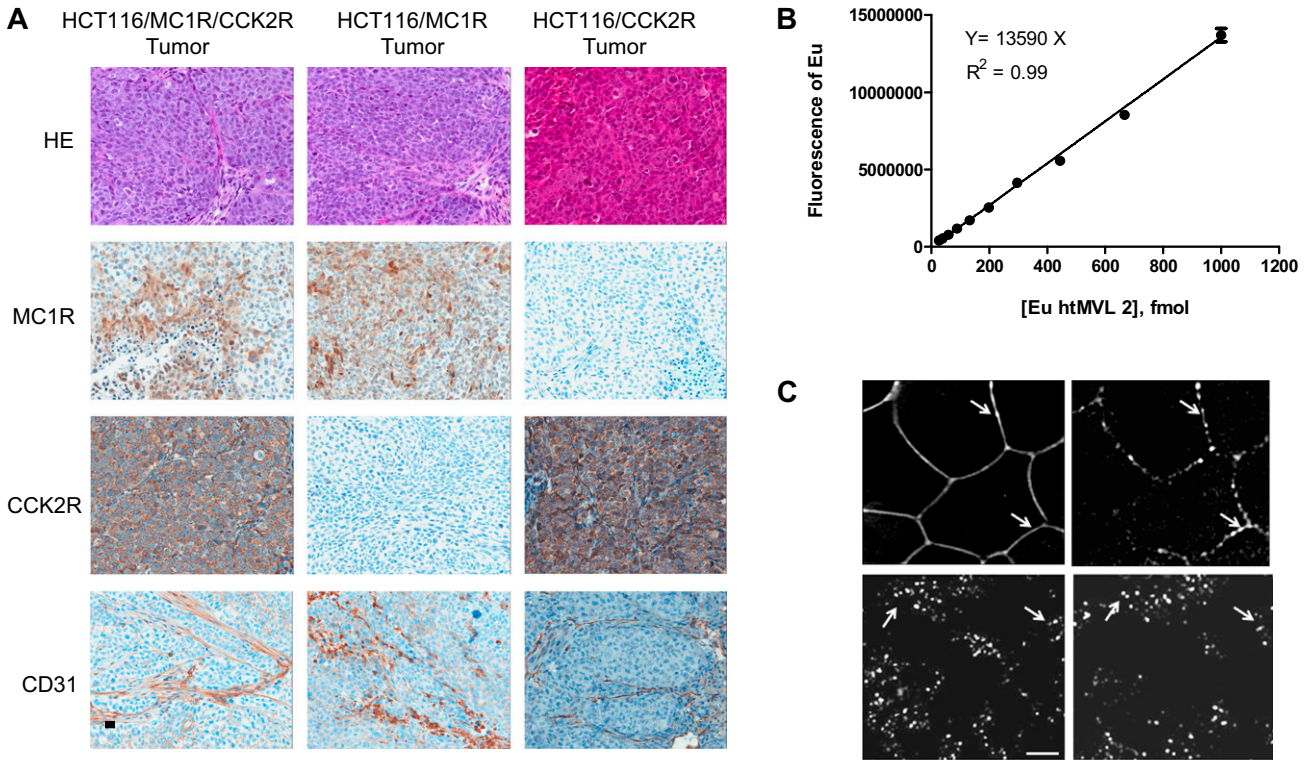

Fig. S4. (*A*) Representative immunohistochemistry staining of target and control tumors. Histological sections from control and target tumors stained with hematoxylin/eosin and anti-MC1R, anti-CCK2R, and anti-CD31 antibodies (*SI Materials and Methods*). MC1R or CCK2R immunostaining was observed in HCT116/MC1R or HCT116/CCK2R tumors, respectively, whereas both MC1R and CCK2R staining was observed in HCT116/MC1R/CCK2R tumors. Comparable CD31 immunostaining was observed in each tumor type, confirming similar vasculature implying uniform ligand delivery. (*B*) Standard curve of Eu-htMVL 2 for in vivo TRF. Standard curve of Eu htMVL 2 was generated by time-resolved fluorescence measurements. Europium fluorescence was determined by various concentrations of htMVL 2 incubated with enhancement solution for 30 min, which demonstrated a linear dynamic range. Each point represents the mean of four independently diluted samples from a single htMVL 2 solution. (*C*) htMVL 1 ligand (50 nM) distribution compared with organelle markers in HEK293 cells stably expressing both MC4R and CCK2R. *C Upper* is FM1-43 plasma membrane label (*Left*) and the ligand (*Right*) at 3 min, and *C Lower* is lysosensor (*Left*) and the ligand (*Right*) at 30 min in live cells. Images were acquired sequentially with ~1 min between image acquisition of the two sets. At 3 mins, all of the ligand is on or at near membrane sites (capping regions). By 30 min, much of the Cy5-tagged ligand is localized in structures coincident with the lysosensor probe (i.e., acidic compartments). Arrows, areas of strong overlap. (Scale bars: *A*, 20 μm; *C*, 10 μm.)

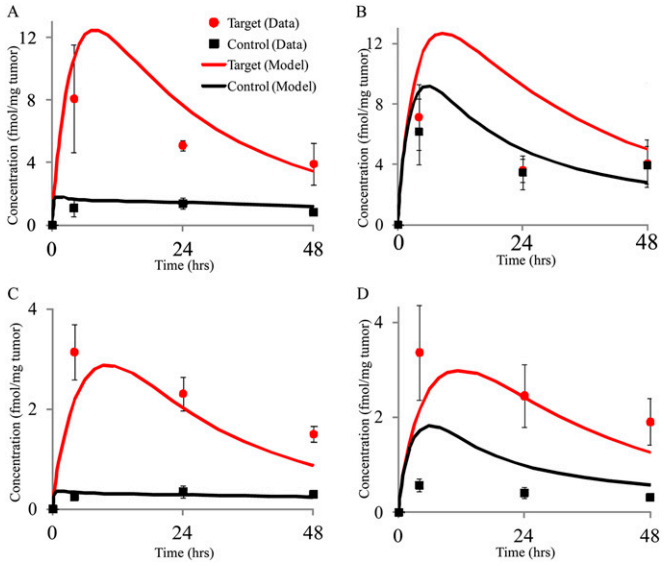

Fig. S5. Mathematical modeling of Eu-htMVL targeting. Mathematical modeling results (solid lines) compared against experiment data (dots). Eu concentration (fmol/mg) in target tumor expresses both MC1R and CCK2R (red) and control tumor expresses either MC1R or CCK2R (black). (*A*) A 2.5 nmol per mouse injection with HCT116/MC1R control cells. (*B*) A 2.5 nmol per mouse injection with HCT116/CCK2R control cells. (*C*) A 0.5 nmol per mouse injection with HCT116/MC1R control cells. (*D*) A 0.5 nmol per mouse injection with HCT116/CCK2R control cells. Error bars are 95% confidence intervals.

Table S1. HPLC and physicochemical data of labeled compounds

Compound no.	Linker	Linear linker length, atoms	Estimated linker length, Å	Molecular formula	Exact mass (calculated)	Mass (observed)	HPLC Rt (% purity)	K′
htMVL 1	PEGO-[PG]$_3$K-PEGO	61	30–70	$C_{174}H_{246}N_{35}O_{45}S_2$	3609.7484	903.6916 $(M+4)^{4+}$	14.6 (96%)	5.1
htMVL 2	PEGO-[PG]$_3$K(Ado)-PEGO	61	30–70	$C_{161}H_{237}EuN_{37}O_{50}$	3641.6352	1215.5575 $(M+3)^{3+}$	15.10 (99%)	5.3

Ado, 8-amino-3,6-dioxaoctanoyl.

Table S2. Eu htMVL 2 content in the HCT116 xenografts (dual receptor tumor versus MC1R tumor)

Tumor ID	Dose, nmol	Eu, counts per mg			Eu,* fmol/mg			% injected dose/g†		
		4 h	24 h	48 h	4 h	24 h	48 h	4 h	24 h	48 h
HCT116/MC1R/CCK2R	2.5	109,957 ± 23,775	69,361 ± 2,378	53,133 ± 9,363	8.09 ± 1.75	5.10 ± 0.17	3.91 ± 0.69	0.32	0.20	0.16
HCT116/MC1R	2.5	14,936 ± 3,754	19,048 ± 2,307	11,267 ± 338	1.10 ± 0.28	1.40 ± 0.17	0.83 ± 0.02	0.04	0.06	0.03
HCT116/MC1R/CCK2R	0.5	42,664 ± 3,828	31,341 ± 2,328	20,448 ± 1,027	3.14 ± 0.28	2.31 ± 0.17	1.50 ± 0.08	0.63	0.46	0.30
HCT116/MC1R	0.5	3,350 ± 153	4,720 ± 768	3,943 ± 380	0.25 ± 0.01	0.35 ± 0.06	0.29 ± 0.03	0.05	0.07	0.06

*Based on the standard curve (Fig. S4*B*), Eu counts per milligram was converted to fmol/mg.
†Based on the standard curve, the injected dose per mouse, 2.5 nmol or 0.5 nmol was converted to Eu counts, 3.4×10^{10} or 6.8×10^9, respectively. Therefore, % injected dose per gram was calculated by the ratio of Eu counts per gram of tissue to Eu counts of the injected dose.

Table S3. Eu htMVL 2 content in the HCT116 xenografts (dual receptor tumor versus CCK2R tumor)

Tumor ID	Dose, nmol	Eu, counts per mg			Eu,* fmol/mg			% injected dose/g†		
		4 h	24 h	48 h	4 h	24 h	48 h	4 h	24 h	48 h
HCT116/MC1R/CCK2R	2.5	96,862 ± 15,257	48,722 ± 5,239	55,367 ± 10,744	7.13 ± 1.12	3.59 ± 0.39	4.07 ± 0.79	0.28	0.14	0.16
HCT116/CCK2R	2.5	83,825 ± 15,124	47,166 ± 7,568	53,811 ± 8,544	6.17 ± 1.11	3.47 ± 0.56	3.96 ± 0.63	0.25	0.14	0.16
HCT116/MC1R/CCK2R	0.5	45,678 ± 6,898	33,277 ± 4,591	25,862 ± 3,416	3.36 ± 0.51	2.45 ± 0.34	1.90 ± 0.25	0.67	0.49	0.38
HCT116/CCK2R	0.5	7,723 ± 1,011	5,576 ± 786	4,147 ± 462	0.57 ± 0.07	0.41 ± 0.06	0.31 ± 0.03	0.11	0.08	0.06

*Based on the standard curve (Fig. S4*B*), Eu counts per milligram was converted to fmol/mg.
†Based on the standard curve, the injected dose per mouse, 2.5 nmol or 0.5 nmol was converted to Eu counts, 3.4×10^{10} or 6.8×10^9, respectively. Therefore, % injected dose per gram was calculated by the ratio of Eu counts per gram of tissue to Eu counts of the injected dose.

Table S4. Eu htMVL 2 content in the kidney and liver

Tissue	Dose, nmol	Eu, counts per mg			Eu,* fmol/mg			% injected dose/g†		
		4 h	24 h	48 h	4 h	24 h	48 h	4 h	24 h	48 h
Kidney	2.5	3,339,186 ± 597,384	3,064,207 ± 67,590	1,338,362 ± 114,792	245.71 ± 43.96	225.48 ± 4.97	98.48 ± 8.45	9.82	9.01	3.94
	0.5	556,966 ± 53,618	571,653 ± 22,000	294,624 ± 14,908	40.98 ± 3.95	42.06 ± 1.62	21.68 ± 1.10	8.19	8.41	4.33
Liver	2.5	33,220 ± 183	51,827 ± 2,516	35,453 ± 3,998	2.44 ± 0.01	3.81 ± 0.19	2.61 ± 0.29	0.10	0.15	0.10
	0.5	9,959 ± 2,267	8,039 ± 761	10,468 ± 135	0.73 ± 0.17	0.59 ± 0.06	0.77 ± 0.01	0.15	0.12	0.15

*Based on the standard curve (Fig. S4*B*), Eu counts per milligram was converted to fmol/mg.
†Based on the standard curve, the injected dose per mouse, 2.5 nmol or 0.5 nmol was converted to Eu counts, 3.4×10^{10} or 6.8×10^9, respectively. Therefore, % injected dose per gram was calculated by the ratio of Eu counts per gram of tissue to Eu counts of the injected dose.

Other Supporting Information Files

Dataset S1 (DOC)